

Nanoscale

Accepted Manuscript



This is an *Accepted Manuscript*, which has been through the Royal Society of Chemistry peer review process and has been accepted for publication.

Accepted Manuscripts are published online shortly after acceptance, before technical editing, formatting and proof reading. Using this free service, authors can make their results available to the community, in citable form, before we publish the edited article. We will replace this *Accepted Manuscript* with the edited and formatted *Advance Article* as soon as it is available.

You can find more information about *Accepted Manuscripts* in the [Information for Authors](#).

Please note that technical editing may introduce minor changes to the text and/or graphics, which may alter content. The journal's standard [Terms & Conditions](#) and the [Ethical guidelines](#) still apply. In no event shall the Royal Society of Chemistry be held responsible for any errors or omissions in this *Accepted Manuscript* or any consequences arising from the use of any information it contains.

COMMUNICATION

SiO₂-Coated Sulfur Particles with Mildly Reduced Graphene Oxide as a Cathode Material for Lithium-Sulfur Batteries

Cite this: DOI:

10.1039/x0xx00000x

Brennan Campbell^a, Jeffrey Bell,^a Hamed Hosseini Bay,^b Zachary Favors,^a Robert Ionescu,^c Cengiz S. Ozkan*^d and Mihrimah Ozkan*^e

Received 00th January 2012,

Accepted 00th January 2012

DOI: 10.1039/x0xx00000x

www.rsc.org/

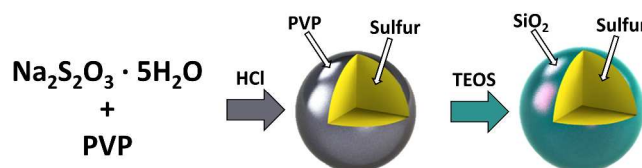
For the first time, SiO₂-coated sulfur particles (SCSPs) were fabricated via a facile two-step wet chemical process for application as a novel lithium-sulfur cathode material. With the addition of mildly reduced graphene oxide (mrGO), SCSPs demonstrate even greater cycling stability, maintaining over 700 mAhg⁻¹ after the 50th cycle.

The invention of rechargeable lithium-ion (Li-ion) battery technology has set the newest paradigm in energy storage over the last several decades. These batteries are becoming well-developed, and have been responsible for powering portable phones, computers, and electric vehicles.¹ While Li-ion battery cathodes presently have a capacity range of ~ 150-200 mAhg⁻¹, the theoretical capacity of lithium-sulfur (Li-S) cathodes is 1675 mAhg⁻¹, and recent research shows that hundreds of cycles at specific capacities of over 700 mAhg⁻¹ is possible.^{2,3} Li-S batteries show great promise in meeting the critical need for EV batteries with high specific capacity, both volumetric and gravimetric. The Li-S system offers other advantages as well; the elements lithium and sulfur offer a relatively low-cost battery due to their light weight and relatively high abundance.^{4,5}

The number of new Li-S battery publications in recent years is growing exponentially, showing the increased interest in addressing the problems with Li-S batteries. However, challenges with the Li-S battery include the low electronic conductivity of sulfur (5 x 10⁻³⁰ S cm⁻¹ at 25°C), poor ionic diffusivity, volumetric expansion during lithiation (~ 80%), and the polysulfide “shuttle” effect, in which the intermediate lithium polysulfides (Li₂S_n, 4 ≤ n ≤ 8) dissolve into the electrolyte.^{6,7,8} Recently, other materials have been introduced into sulfur cathodes, many of which have properties that enhance cathode performance in ways that carbon cannot. For instance, TiO₂ and several other oxide nanostructures have been demonstrated as beneficial additions to sulfur cathodes, due to their inertness to redox reactions and extraordinary polysulfide adsorbing properties.^{9,10} In many cases SiO₂ is termed a “polysulfide reservoir,” as in the work done by Ji et. al., wherein SBA-15 mesoporous silica was used as an additive in a mesoporous carbon/sulfur composite for a lithium-

sulfur cathode structure. In this work it was demonstrated that the small amount of SiO₂ additive was necessary for trapping polysulfides and then readily desorbing them during electrochemical reduction/oxidation.¹¹ In addition, the increased stability shown in the cycling of this cathode composite was attributed to the mesoporous structure of the SiO₂, inhibiting diffusion of the polysulfide anions. Besides SiO₂, other oxides have been shown to stabilize soluble polysulfide species, including Al₂O₃ and La₂O₃, often incorporated into nanocomposites with graphene or graphene oxide (GO).^{23,24} The battery performance of a sulfur-silica core-shell structure has, until now, yet to be explored.

Figure 1. A schematic illustration of the two-step wet chemical synthesis of SCSPs, showing the starting materials sodium thiosulfate pentahydrate and PVP (a), the formation of PVP/CSPPs

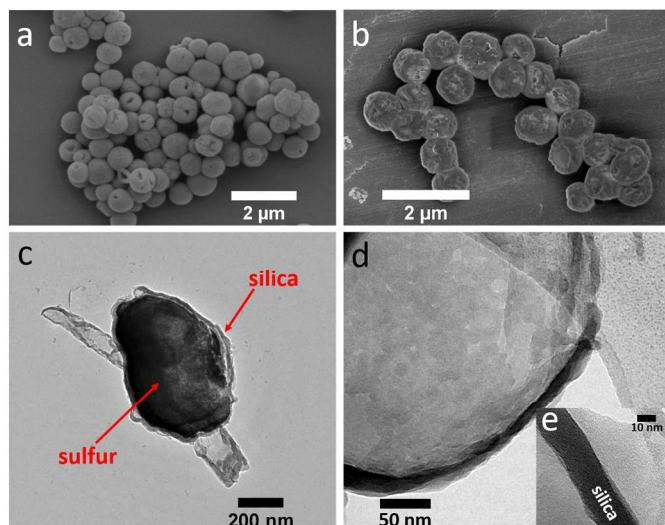


after HCl addition (b) and finally the SCSPs after addition of TEOS solution (c).

Herein, we report the facile wet synthesis of SiO₂-coated sulfur particles (SCSPs), and assess this novel material as a possible Li-S battery cathode. The general synthesis of SCSPs is outlined in Fig. 1, and the synthesis was performed as follows: A 100 mL aqueous solution of Na₂S₂O₃·5H₂O (1g) and polyvinylpyrrolidone (PVP) (20 mg, 55,000 MW), an amphiphilic surfactant polymer, was prepared. While mildly stirring the solution, 0.80 mL concentrated HCl was added dropwise. The reaction requires two hours for completion, although a white cloudy precipitate can be observed almost instantly. During this time, thiosulfate ions decompose into elemental sulfur

(S₈), which forms particles that are coated with PVP. After two hours, the contents of the reaction vessel were centrifuged for 10 minutes at 3.6 krpm, and resuspended in a 0.05 wt% solution of PVP.¹² The suspension was again centrifuged for 10 minutes at 3.6 krpm, and this wash/centrifuge process was done two more times using deionized water (DI H₂O). The washed PVP-coated sulfur particles (PVPCSPs) were suspended in 20 mL DI H₂O and set aside. Next, a modified Stöber process was used to coat the sulfur particles with silica (SiO₂).^{13,14,15} In this process, a solution of tetraethyl orthosilicate (TEOS) was first prepared by adding 20 μL TEOS to 20 mL methanol (MeOH). In a flask, 80 mL MeOH and 2 mL 30% ammonia (NH₃) were combined and stirred vigorously. While stirring, the 20 mL PVPCSP suspension was transferred dropwise to the NH₃ solution. The TEOS solution was then added to the reaction vessel dropwise, adding 5 mL every 30 minutes until there was no remaining TEOS solution. The reaction was stirred for 17 hours, then centrifuged and washed several times with DI H₂O and isopropyl alcohol (IPA). The reaction was optimized to these conditions by varying ageing time for the Stöber process (12-24 hours), and the amount of TEOS added (10-30 μL).

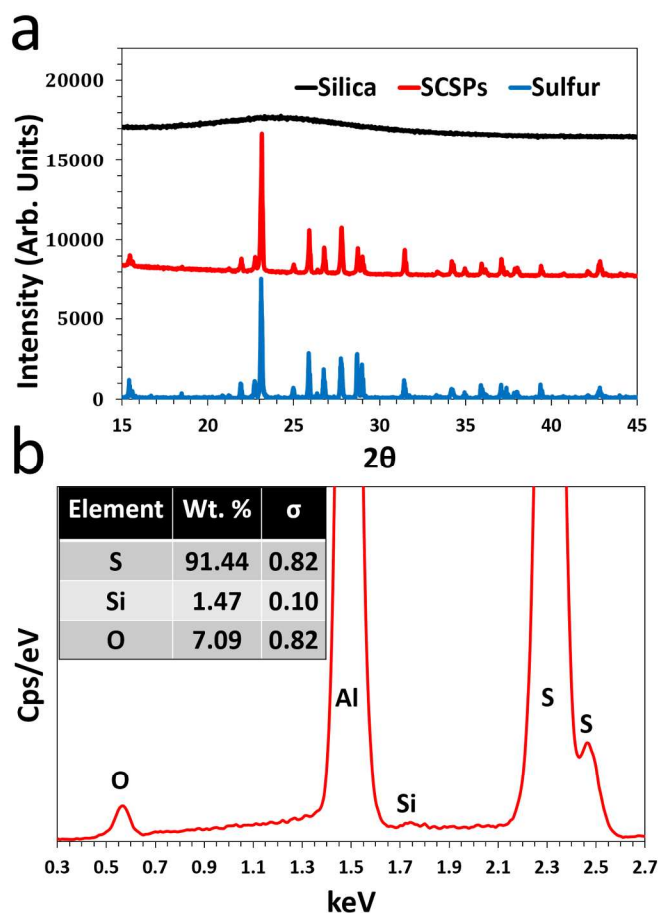
For addition of mildly reduced graphene oxide (mrGO), Hummer's method was first used to prepare graphene-oxide (GO).¹⁶ Next, 20 mg SCSPs were suspended in 10 mL ethanol (EtOH), and was kept stirring. A separate suspension of 6 mg GO in 3 mL DI H₂O was also prepared, and then slowly added to the SCSP suspension while stirring. The reaction vessel was then placed in an ice bath, and 16 μL hydrazine was added for the partial reduction. This reaction was allowed to stir at 0°C for 24 hours, after which the product was washed repeatedly with DI H₂O and dried under



vacuum for 24 hours at 60°C.

Figure 2. SEM images of PVP-coated sulfur particles (a), SCSPs (b), and TEM images of an isolated SCSP, still containing sulfur (c), the remaining silica shell after sulfur escape (d), and HRTEM of the silica shell showing its amorphous nature (e).

Morphologies of the PVPCSPs and SCSPs were studied using scanning electron microscopy (SEM), and are seen in Fig. 2a and 2b, respectively. In Fig. 2a, PVPCSPs are shown to have a spherical shape, with a diameter of about 700-800 nm. Some smaller particles also tend to form during the synthesis is most likely due to small



changes in reaction conditions. Under the SEM beam, the PVP coatings distort, revealing their core-shell type structure. Fig. 2b **Figure 3.** Spectral data including XRD of amorphous silica, SCSPs, and elemental sulfur (a) and EDS of SCSPs, including corresponding relative weight percentages (b).

exhibits the SCSPs on an aluminum substrate. The diameter of the SCSPs are generally greater than the PVPCSPs, while the SiO₂ coatings appear bumpy and somewhat uneven at the surface. This uneven surface is possibly attributed to a degree of compositional inhomogeneity in the deposited silica coatings.¹⁷ As a consequence, many SCSPs tend to assume a potato-like morphology rather than a perfect spherical morphology, although most tend to remain relatively spherical. Besides the bumps on the surface, we see from TEM analysis in Fig. 2 that the SiO₂ renders as a thin film on the surface of the sulfur particles. Fig. 2c captures a smaller potato-shaped SCSP, differentiating the sulfur core from the SiO₂ shell. The particle is resting on top of a SiO₂ nanotube, which tend to form when there is excess PVP that carries over from the PVPCSP synthesis. TEM of the silica shell is shown in Fig. 2d, allowing a view of the continuous coating without sulfur. This image is the results of the electron beam causing the sulfur to react and escape the structure, giving valuable information about the shell alone. HRTEM on the silica shell (Fig. 2e) confirms that the silica is amorphous. On average, the thickness of the SiO₂ shell is about 20 nm, although the thickness increases near the bumps. The amorphous nature of the SiO₂ coating was also confirmed with HRTEM in Fig. 2e. Evidently, there is a relatively high degree of control over the size and

morphology of the novel SCSP material, making it an ideal system to electrochemically characterize as a Li-S cathode material. Furthermore, point ID energy dispersive x-ray

while allowing Li^+ diffusion. During battery fabrication we have found that, rather than solely including carbon black (CB) as a conductive additive, the addition of mildly reduced graphene oxide

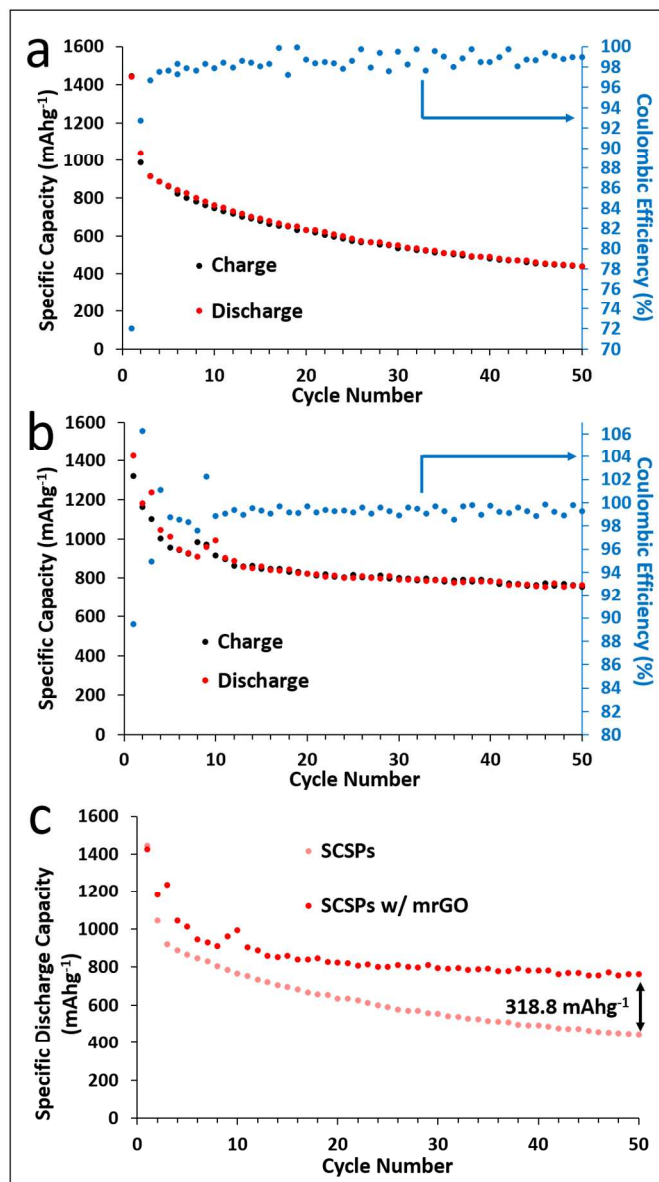
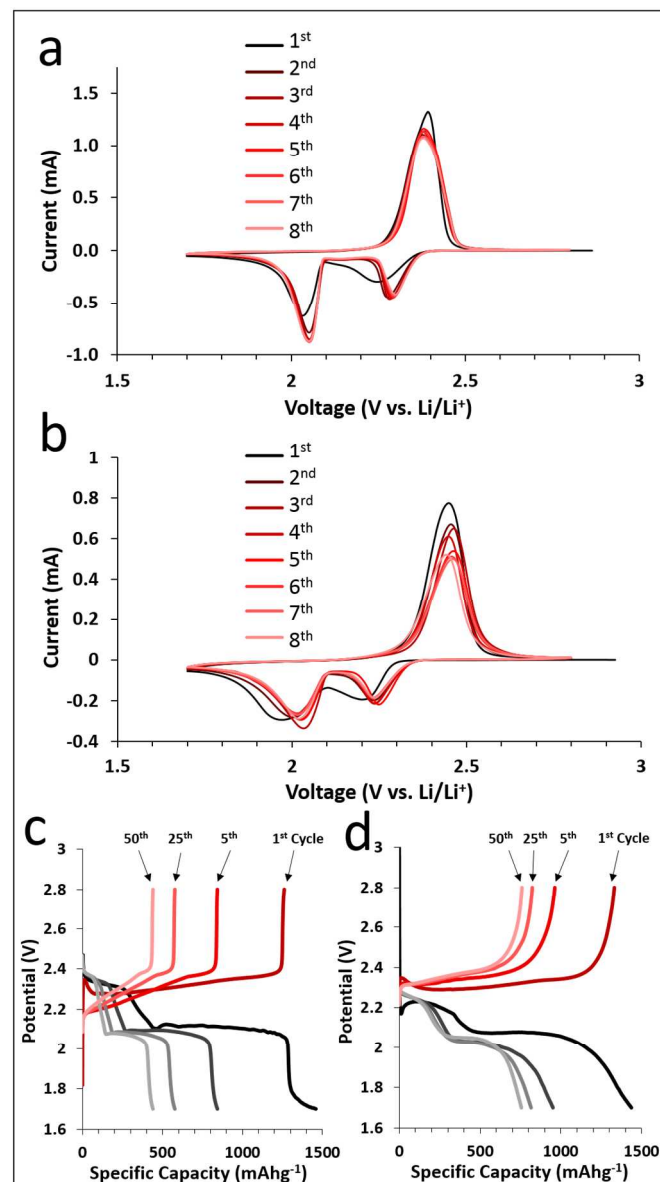


Figure 4. Cyclability plots for SCSPs (a) and for SCSPs with mrGO as an additive (b), and the discharge cycle capacity comparison of SCSPs with and without mrGO to 50 cycles (c).

spectroscopy (EDS) confirmed the presence of both elemental sulfur and silica in SCSPs, while the prevailing presence of sulfur with respect to silica in the SCSP cathode is evidenced by the XRD spectrum of SCSPs in comparison to amorphous SiO_2 and sulfur, seen in Fig. 3a. The Al peak in EDS results from the aluminum substrate used to prevent skewing of the presence of Si.

The amorphous thin-layer SiO_2 shell surrounding the sulfur cores inhibits the polysulfide shuttle effect, acting as an adsorbent barrier and polysulfide reservoir. The polysulfide shuttle effect tends to hinder typical carbon-sulfur cathode structures and they may experience active material loss. SiO_2 has the inherent ability to surface-adsorb polysulfide species that are soluble in the electrolyte, which deters the loss of electrochemically active sulfur over numerous cycles.¹¹ In this design, the SiO_2 shell carries out this task,



(mrGO) significantly improves the cyclability of the cathode, boosting its

Figure 5. Cyclic voltammetry for SCSPs (a) and for SCSPs with mrGO as an additive (b), and voltage profiles of SCSPs (c) and SCSPs with mrGO (d).

discharge capacity by over 300 mAhg⁻¹ after 50 cycles. mrGO was chosen as a necessary ingredient for the cathode composite due to its ability to wrap its sheets around particles and form a more interconnected conductive network. Thus, it is an equally essential part of the design of this cathode, due to its SiO_2 -harnessing action. CB alone would not have provided this conductive sink, which poses a problem for this cathode material composed of one insulator (sulfur) coated with another insulator (SiO_2). As the structure becomes damaged over time, the mrGO acts as a conductive net, contains the structures, and also has polysulfide-trapping properties.

Thus, there are several modes of action by which the addition of mrGO helps to improve the cycle stability of SCSPs.

The sulfur content of as-synthesized SCSPs was about 90 wt% based on EDS data from several syntheses (Fig. 3b). For all cyclability plots, the first cycle was run at a C/50 rate, based on the theoretical capacity of 1675 mAhg^{-1} , while each subsequent cycle was run at a C/10 rate. This slow current cycling was necessary due to the highly insulating nature of the SCSP structure. Cyclic voltammetry (CV) curves were obtained using a scan rate of 0.1 mVs^{-1} . After 50 cycles, the SCSPs maintain a respectable specific discharge capacity of 444.4 mAhg^{-1} (Fig. 4a), which is still significantly higher than that of materials used in industry today. The conversion $\text{S}_8 \rightarrow \text{Li}_2\text{S}$ is repeatedly allowed to proceed reversibly for several cycles, indicated by the Coulombic efficiency stabilizing at $\sim 99\%$. However, the capacity decay over the first 50 cycles is still substantial, with an average specific capacity loss of 12.2 mAhg^{-1} per cycle from cycle 2 to 50. The CV curve for SCSPs, shown in Fig. 5a, highlights typical lithiation and delithiation peaks for Li-S cathodes, where as expected, lithiation decreases slightly and then stabilizes after cycle 2. This is owed to the ultra-low current density for cycle 1 and the thin SiO_2 coating, which are both thought to encourage the formation of a stable SEI layer.^{18,19} As evidenced from the cycling data for SCSPs, capacity fading was still fairly significant for the SCSP cathode, and is most likely due to the encapsulation of an extremely electronically insulating material (S_8) with another insulating material (SiO_2 , band gap $\sim 9 \text{ eV}$).²⁰ The capacity loss experienced with SCSPs alone was the impetus for the addition of mrGO to the cathode mixture, and study thereof. According to Fig. 4b, the capacity decay of SCSPs is markedly improved with the addition of mrGO. From cycles 2 through 50, an average capacity loss per cycle was only 8.6 mAhg^{-1} was experienced, with an improved Coulombic efficiency of $\sim 99.3\%$. The CV curve also shows excellent stability of the mrGO-enhanced cathode, exhibiting a more diverse range of redox peaks compared to that of SCSPs alone (Fig. 5b). While the lithiation and delithiation peaks stabilize after the first few cycles, there is also a slight up-field shift in their redox potentials after cycle 1; this shift and subsequent stabilization is likely due to the entrapment of SiO_2 and polysulfides between mrGO sheets. With mrGO as an additive, the 50th discharge of SCSPs showed a specific capacity of 763.2 mAhg^{-1} . Thus, as depicted in the comparison in discharge capacities in Fig. 4c, a result of mrGO and CB as combined conductive additives rather than CB alone was a 318.8 mAhg^{-1} boost, an enormous benefit. It is hypothesized that these benefits come from the partial wrapping of the SCSP particles, which allows for intimate contact of conductive medium, rather than small CB particles being randomly dispersed throughout the mixture. An added benefit is the polysulfide shuttle-inhibiting properties of the mrGO; this becomes crucial as the SCSP structure breaks down over a number of cycles.

Notably, sulfur is demonstrating its 3 major voltage plateaus in the charge-discharge plots; the 1st and smallest plateau is derived from the solid Li_2S_8 species (2.4-2.3V), the 2nd and sharpest plateau from the conversion of Li_2S_8 to the soluble Li_2S_6 species (2.3-2.1V), and finally the longest plateau from the soluble species $\text{Li}_2\text{S}_{6 \times 2}$ (2.1-2.0V).^{21,22} The discharge/charge voltage profiles of SCSPs and SCSPs with mrGO were obtained for analyzing the voltage plateau regions. The plateaus of the 1st cycle of SCSP cathode are in good agreement with the charge and discharge peak of its respective CV curve (shown in Fig. 5c), with the primary operating region between 2.3 and 2.4V for charging and 2.0 and 2.3V for discharging. The later charges, however, begin experiencing a broader voltage window. For example, the 5th, 25th and 50th charges operate between 2.2 and 2.4V, while the discharges remain in the same operating window. As illustrated in Fig. 5d, when mrGO is added, an extended

voltage plateau is gained for later cycles, with the discharge/charge capacity stabilizing at about 700 mAhg^{-1} for the 50th cycle, in contrast to about 400 mAhg^{-1} for SCSPs alone. The voltage plateaus for the mrGO-enhanced SCSPs also agree with its respective CV curve, and there is also a greater curvature to the plateaus, lending additional capacity to higher voltages. An auxiliary effect of the mrGO additive is the absence of operational voltage reduction, as is seen in the solely SCSP cathode.

The assembly of the SCSP-based coin cell batteries involved mixing a 6:3:1 weight ratio of SCSPs, CB, and polyvinylidene fluoride (PVdF) using a mortar and pestle. A slurry was made with N-Methyl-2-pyrrolidone (NMP), which was cast onto high-purity aluminum foil current collectors and placed in a vacuum oven at 60°C overnight to dry. CR2032-type coin cells were then fabricated with the SCSPs/CB/PVdF composite as the working electrode, microporous polypropylene as the separator (Celgard 2300), and lithium metal foil as the counter electrode. The electrolyte used was 1M lithium bis(trifluoromethanesulfonyl)imide (LiTFSI) in a 1:1 vol. ratio of 1,3-dioxolane (DOL) and 1,2-dimethoxyethane (DME), and lithium nitrate (LiNO_3) as a lithium-passivating additive at a concentration of 0.5 wt%. Cells were prepared in an Ar-filled VAC Omni-lab glovebox, and were tested vs. lithium from 1.7 to 2.8V on an Arbin BT2000. CV data was collected using a Bio-logic VMP3 with a scan rate of 0.1 mVs^{-1} . Scanning electron microscopy characterization was performed using an FEI Nova Nano450SEM, an FEI XL30 SEM, and transmission electron microscopy was carried out using a Philips CM300 TEM.

In this study, silica-coated sulfur particles (SCSPs) were synthesized and characterized as a cathode material for Li-S batteries. This novel core-shell structure was fabricated in a facile 2-step wet chemical synthesis. The SCSP cathode showed superior cycling stability when coupled with mrGO as an additive, improving the capacity retention after 50 cycles from 440.8 mAhg^{-1} without mrGO to 763.2 mAhg^{-1} with mrGO. The electrochemical data also shows reduced capacity fading over 50 cycles, from 12.2 mAhg^{-1} per cycle without mrGO to 8.6 mAhg^{-1} per cycle with mrGO. During cycling, SCSPs are understood to fracture and release active material (S_8), and mrGO helps to contain the ruptured particles, thereby improving cycling stability. By the 50th cycle, SCSPs experienced a 318.8 mAhg^{-1} boost in specific discharge capacity with the addition of mrGO. These improvements are attributed to the polysulfide inhibiting effects of SiO_2 as well as the host of benefits provided by mrGO, similar to other work.^{23,34} Thus, SCSPs with the addition of mrGO show great promise in the application of low-cost, high energy density battery systems for portable electronics and EVs. Further investigation is needed on the SCSP cathode system, expressly into the silica shell pulverization during cycling.

The authors thank Winston Global Energy Center for partially supporting this work, Krassimir Bozhilov and Mathias Rommelfanger in the Central Facility for Advanced Microscopy and Microanalysis (CFAMM) at UC Riverside, for their guidance with TEM. They also acknowledge Lauro Zavala for artistic contributions.

Notes and references

* Corresponding authors: mihri@ece.ucr.edu; cozkan@enr.ucr.edu

^a B. Campbell, J. Bell, Z. Favors, Materials Science and Engineering Program, University of California, Riverside, CA 92521 (USA).

^b H. H. Bay, Department of Mechanical Engineering, University of California, Riverside, CA 92521 (USA).

^c R. Ionescu, Department of Chemistry, University of California, Riverside, CA 92521 (USA).

^d C. S. Ozkan, Materials Science and Engineering Program, Department of Mechanical Engineering, University of California, Riverside, CA 92521 (USA). cozkan@engr.ucr.edu

^e Mihrimah Ozkan, Department of Electrical Engineering, Materials Science and Engineering Program, Department of Chemistry, University of California, Riverside, CA 92521 (USA). mihri@ece.ucr.edu

- 23 M. Yu, W. Yuan, C. Li, J. Hong, and G. Shi, *J. Mater. Chem. A*, 2014, **2**, 7360-7366.
- 24 F. Sun, J. Wang, D. Long, W. Qiao, L. Ling, C. Lv, and R. Cai, *J. Mater. Chem. A*, 2013, **1**, 13283-13289.

- 1 Y. Su and A. Manthiram, *Chem. Commun.*, 2012, **48**, 8817-8819.
- 2 G. Ma, Z. Wen, J. Jin, Y. Lu, X. Wu, M. Wu, and C. Chen, *J. Mater. Chem.*, 2014, **2**, 10350-10354.
- 3 J. Wang, L. Yin, H. Jia, H. Yu, Y. He, J. Yang, and C. W. Monroe, *ChemSusChem*, 2014, **7**, 563-569.
- 4 C. Liang, N. Dudney, and J. Howe, *Chem. Mater.*, 2009, **21**, 4724-4730.
- 5 B. Zhang, X. Qin, G. R. Li, and X. P. Gao, *Energy Environ. Sci.*, 2010, **3**, 1531-1537.
- 6 Y. Yang, G. Zheng, and Y. Cui, *Chem. Soc. Rev.*, 2013, **42**, 3018-3032.
- 7 A. Fedorkova, R. Orinakova, O. Cech, and M. Sedlarikova, *Int. J. Electrochem. Sci.*, 2013, **8**, 10308-10319.
- 8 W. Li, Q. Zhang, G. Zheng, Z. Seh, H. Yao, and Y. Cui, *Nano Lett.*, 2013, **13**, 5534-5540.
- 9 Q. Li, Z. Zhang, K. Zhang, L. Xu, J. Fang, Y. Lai, and J. Li, *J. Solid State Electrochem.*, 2013, **17**, 2959-2965.
- 10 B. Ding, L. Shen, G. Xu, P. Nie, and X. Zhang, *Electrochim. Acta*, 2013, **107**, 78-84.
- 11 X. Ji, S. Evers, R. Black, and L. Nazar, *Nat. Commun.*, 2011, **2**, 1-7.
- 12 H. Wang, Y. Yang, Y. Liang, J. T. Robinson, Y. Li, A. Jackson, Y. Cui, and H. Dai, *Nano Lett.*, 2011, **11**, 2644-2647.
- 13 W. Rho, H. Kim, S. Kyeong, Y. Kang, D. Kim, H. Kang, C. Jeong, D. Kim, Y. Lee, and B. Jun, *J. Ind. Eng. Chem.*, 2014, **20**, 2646-2649.
- 14 C. Graf, D. L. J. Vossen, A. Imhof, and A. van Blaaderen, *Langmuir*, 2003, **19**, 6693-6700.
- 15 N. R. Jana, C. Earhart, and J. Y. Ying, *Chem. Mater.*, 2007, **19**, 5074-5082.
- 16 S. Stankovich, D. A. Dikin, R. D. Piner, K. A. Kohlhaas, A. Kleinhammes, Y. Jia, Y. Wu, S. T. Nguyen, and R. S. Ruoff, *Carbon*, 2007, **7**, 1558-1565.
- 17 Y. J. Wong, L. Zhu, W. S. Teo, Y. W. Tan, Y. Yang, C. Wang, and H. Chen, *J. Am. Chem. Soc.*, 2011, **133**, 11422-11425.
- 18 J. Shim and K. A. Striebel, *J. Power Sources*, 2003, **119-121**, 955-958.
- 19 L. Su, Z. Zhou, and M. Ren, *Chem. Commun.*, 2010, **46**, 2590-2592.
- 20 D. Waroquiers, A. Lherbier, A. Miglio, M. Stankovski, S. Ponce, M. J. T. Oliveira, M. Giantomassi, G. Rignanese, and X. Gonze, *Phys. Rev. B*, 2013, **87**, 075121.
- 21 Y. Yin, S. Xin, Y. Guo, and L. Wan, *Angew. Chem. Int. Ed.*, 2013, **52**, 13186-13200.
- 22 M. Song, E. J. Cairns, and Y. Zhang, *Nanoscale*, 2013, **5**, 2186-2204.

Graphical Abstract

SiO₂-Coated Sulfur Particles with Mildly Reduced Graphene Oxide as a Cathode Material for Lithium-Sulfur Batteries

Brennan Campbell, Jeffrey Bell, Hamed Hosseini Bay, Zachary Favors, Robert Ionescu, Cengiz S. Ozkan* and Mihrimah Ozkan*

For the first time, SiO₂-coated sulfur particles (SCSPs) were fabricated via a facile two-step wet chemical process for application as a novel lithium-sulfur cathode material. With the addition of mildly reduced graphene oxide (mrGO), SCSPs demonstrate even greater cycling stability, maintaining over 700 mAhg⁻¹ after the 50th cycle.

